PNAS RESEARCH ARTICLE | SUSTAINABILITY SCIENCE OPEN ACCESS

Impact of solar geoengineering on temperature-attributable mortality

Anthony Harding[a,1], Gabriel A. Vecchi[b,c], Wenchang Yang[b], and David W. Keith[d]

Affiliations are included on p. 9.

Edited by Scott Barrett, Columbia University, New York, NY; received February 5, 2024; accepted October 2, 2024

Decisions about solar geoengineering (SG) entail risk–risk tradeoffs between the direct risks of SG and SG's ability to reduce climate risks. Quantitative comparisons between these risks are needed to inform public policy. We evaluate idealized SG's effectiveness in reducing deaths from warming using two climate models and an econometric analysis of temperature-attributable mortality. We find SG's impact on temperature-attributable mortality is uneven with decreases for hotter, poorer regions and increases in cooler, richer regions. Relative to no SG, global mortality is reduced by over 400,000 deaths annually [90% CI: (−1.2 million,2.7 million)] for cooling of 1 °C from 2.5 °C above preindustrial in 2080. We find no evidence that mortality reduction achieved by SG is smaller than the reduction from equivalent cooling by emissions reductions. Combining our estimates with existing estimates of sulphate aerosol injection direct mortality risk from air quality and UV-attributable cancer enables the first quantitative risk-risk comparison of SG. We estimate with 61% probability that the mortality benefits of cooling outweigh these direct SG risks. We find the benefits outweigh these risks by 13 times for our central estimates, or 4 deaths per 100,000 per 1 °C per year [90% CI: (−11,23)]. This is not a comprehensive evaluation of the risk–risk tradeoffs around SG, yet by comparing some of the most consequential impacts on human welfare it is a useful first step. While these findings are robust to a variety of alternative assumptions, considerable uncertainties remain and require further investigation.

solar geoengineering | human mortality | risk–risk analysis

Significance

Solar geoengineering (SG) can cool the climate—the hard question is how its risks compare with its benefits? Using climate model simulations of idealized SG and data-driven of temperature-attributable mortality, we estimate that, in a world 2.5 °C warmer than preindustrial, 1 °C of global-average cooling by SG reduces mortality by over 400,000 deaths annually by 2080, with a possible range from −1.2 million to 2.7 million deaths annually. Mortality decreases in many hot, poor regions and increases in some cold, rich regions. We estimate the mortality benefits of reducing temperatures outweigh risks from air pollution and from ozone loss by 13 times for our central estimates, with a 61% probability the benefits exceed the risks. Uncertainty remains significant, highlighting the need for further research on SG's trade-offs.

Temperature-attributable mortality is a major risk of climate change. A recent study found that annual temperature-attributable mortality would increase by about 14 deaths per 100,000 by the end of the 21st century for a moderate emissions scenario, 85 for a high emissions scenario (1). Some studies have found that temperature-attributable mortality is the largest monetized cost of climate change, composing around half of the total costs that have been quantified and monetized (2, 3). Mortality risk is not evenly distributed: the largest increases in temperature-attributable mortality are concentrated in the hottest and poorest regions of the world (1).

Decisions about SG should be informed by comprehensive and quantitative risk–risk analyses (4–6) that weigh SG's capacity to moderate climate risks against the risks its use entails. Despite the importance of mortality risk and growing interested in SG, there is little research that quantifies the mortality impacts of SG. Eastham et al. (7) quantify the impact of stratospheric sulfate aerosol on ground level ozone, particulate matter, and ground-level UV-B flux. Other research analyzes the human mortality impact of SG through its effect on heat stress (8) and malaria (9); however, these analyses do not quantify impacts.

We estimate solar geoengineering's (SGs) impact on temperature-attributable mortality and take a small step toward a more comprehensive risk–risk analysis SG. The naïve expectation is that SG would reverse the impact of CO_2-driven warming on temperature-attributable mortality. Yet, while SG could be used to reduce global temperatures, it is—at best—an imperfect substitute for CO_2 emissions cuts; a climate with CO_2 warming offset by some SG will not be the same as a climate with the same average temperature achieved by CO_2 controls (10).

Where possible, we normalize our results by the change in global average temperature, a common normalization in the literature. This minimizes the need to anchor our results to an arbitrary assumption about the amount of SG that might be deployed, though it assumes linear scaling of local impact to global temperature. This normalization also allows us to test the naïve expectation that SG's impact on temperature-attributable mortality would be the same as if the change in temperature had been driven by a change in CO_2.

Author contributions: A.H. and D.W.K. designed research; A.H. and W.Y. performed research; G.A.V. and W.Y. contributed new reagents/analytic tools; A.H. analyzed data; A.H., G.A.V., W.Y., and D.W.K. edited and revised paper; and A.H. and D.W.K. wrote the paper.

The authors declare no competing interest.

This article is a PNAS Direct Submission.

[1]To whom correspondence may be addressed. Email: tony.harding@gatech.edu.

This article contains supporting information online at https://www.pnas.org/lookup/suppl/doi:10.1073/pnas.2401801121/-/DCSupplemental.

Published December 17, 2024.

Roughly uniform SG might employ a range of methods, from various stratospheric aerosols to cirrus thinning to space-based methods. The most technically feasible method today is to add sulfur to the stratosphere (11). Our judgment is that the most policy-relevant question for SG is how a moderate amount of SG might supplement a moderate emissions reduction scenario—e.g. use of SG to gradually reduce temperatures to a peak reduction of order 1 °C in the latter half of the century. Given the uncertainty about technology and deployment strategy, our primary climate simulation uses solar constant reduction as a proxy for uniform SG. Later, we explore the consequences of this choice by using an alternative climate model simulation in which sulfate aerosol is injected with a control algorithm optimized to maintain multiple temperature targets.

In a first step toward a quantitative risk–risk comparison around SG, we compare our estimates of the effect of SG on temperature-attributable mortality to prior estimates of the direct risk of SG on mortality through impacts on air quality and UV-attributable cancer. This is far from a comprehensive risk–risk assessment of SG. Yet it is significant because particulate matter and the impacts of warming on temperature-attributable mortality are among the most important paths by which pollution impacts human welfare.

Results

We first use the Geophysical Fluid Dynamics Laboratory Forecast-oriented Low Ocean Resolution (GFDL/FLOR) model (12). We chose a model with a relatively high (50 km) spatial resolution and simulate time-invariant climate conditions to better represent temperature extremes and reduce uncertainties driven by internal variability (13, 14). We then compare these results with lower-resolution time-varying simulations. Relative to a control that simulates 1990s climate conditions for 300 y, we model 200 years of response to CO_2 doubling ($2xCO_2$) and 200 y of $2xCO_2$ offset by a solar constant reduction of 1.7%, chosen to restore net radiative forcing ($2xCO_2$&SG) (*SI Appendix*, Fig. S1 and *Methods*). For our analyses below we only use the final 100 years of each experiment to allow for equilibration. Comparing global mean surface temperature across climate experiments, this gives 2.2 °C of cooling from SG, partially offsetting 2.5 °C of warming.

We quantify the impact of SG on temperature-attributable mortality by applying econometric estimates of the historical relationship between temperature and mortality from Carleton et al. (1). Their analysis uses subnational data for 40 countries to estimate nonlinear exposure-response functions with heterogeneity across age groups and across regions based on their historical climate and income (*SI Appendix*, Fig. S2). By incorporating both climate and income interactions, they allow for these exposure-response functions to evolve with income growth and adaptations to changing climate. Following their approach, we estimate temperature-attributable mortality for 24,378 regions, each around the size of a US county, spanning the globe (*Methods*).

Temperature-Attributable Mortality Projections. If SG were ever used, the timing of deployment and the amount cooling—both how much aerosol is deployed and how it is distributed—is a nonobvious policy choice. To apply the empirical framework of Carleton et al. (1) with the time-invariant FLOR climate model simulations, we consider SG deployment in 2080, applying income and population levels for Shared Socioeconomic Pathway 3 (SSP3) in 2080. For each climate model experiment, we assume that impact regions have adapted to their climate for that respective simulation. That is, impact regions are adapted to 1990 s climate for the control simulation, adapted to the $2xCO_2$ climate for the $2xCO_2$ experiment simulation, and adapted to the $2xCO_2$&SG climate for the $2xCO_2$&SG experiment simulation. This provides a lower-bound estimate that conceptually represents the long-run impact from changes in steady-state climate. Later and in the appendix, we analyze the effect of relaxing these assumptions about income growth and climate adaptation. Later, we also consider an alternative time-varying climate model that can account for changes in climate and income over time following Carleton et al.'s approach. We focus only on physical mortality rate impacts and thus do not include adaptation costs as considered by Carleton et al. (1). Including adaptation costs would increase the estimated impact of SG.

To further avoid anchoring to an arbitrary SG scenario, we normalize our estimates by the change in global mean temperature.[*] This provides a first-order approximation that allows one to scale the impact of SG from prior work on the impact of reduced CO_2, e.g. for use in Integrated Assessment Models (IAMs). Of course, given the nonlinear convex relationship between global mean temperature and temperature-attributable mortality, the impact of cooling depends on both the initial reference temperature and the amount of cooling. We also compare the normalized impact of SG to the counterfactual impact of emissions cuts.[†] This is not because we believe SG should substitute for CO_2 emissions reductions but to understand the response to SG as a deviation from the response to temperature change due to CO_2 alone. We account for uncertainty through Monte Carlo simulation, sampling across climate variability and statistical uncertainty (*Methods*).

Comparing the $2xCO_2$&SG and $2xCO_2$ experiments, for cooling of 2.2 °C from 2.5 °C above preindustrial in 2080, we find that SG reduces global average temperature-attributable mortality rate by 8 [90% CI: (−23,51)], where we will consistently express *mortality rates* as deaths per 100,000 per year. Normalized, the change in average mortality rate reduction is 4 per 1 °C [90% CI: (−10,23)], which is around 0.5% of the 2019 global all-cause mortality rate and 0.3% of the projected end-of-century global all-cause mortality rate (15). Thus, for a global population in 2080 of around 11.7 billion under SSP3, a cooling of 1 °C from SG reduces temperature-attributable mortality by around 400,000 deaths [90% CI: (−1.2 million,2.7 million)].

SG's impact varies strongly with latitude (Fig. 1 *A* and *C*). Hot regions generally benefit from cooling while mortality risk increases in colder regions. Per degree of SG cooling, for example, mortality rate in Delhi decreases by 4 [90% CI: (−14,45)] while in Boston increases by 14 [90% CI: (−16,49)]. We find that, on average, SG reduces mortality rates for 65% of the global population and increases it for 35% (*SI Appendix*, Table S1). Because the oldest age group (65+) is the most sensitive to temperature-attributable mortality (*SI Appendix*, Fig. S2), they compose most of both global and regional mortality risk impacts—both positive and negative—followed by the youngest age group (<5).

Globally, we compare the mortality risk impact of SG to emissions reductions and find that, normalized per degree of cooling, SG reduces mortality rates by 1.4 [90% CI: (−1.0,3.9)] more than emissions reductions. Regionally, we find that, on average, 77% of the global population benefits more from cooling with SG while 23%

[*] In *SI Appendix*, Figs. S12 and S13, we instead normalize by change in mean surface temperature in each respective impact region rather than global mean surface temperature. We thank an anonymous reviewer for the idea for this analysis.

[†] Note, to model the impact of emissions reductions we compare the high CO_2 concentration $2xCO_2$ climate model simulation to the control climate model simulation. In this way, what we measure is the *counterfactual* effect of CO_2 emissions reductions. This comparison assumes that the climate impacts of CO_2 concentration are quasi-linear and reversible. This could also represent the effect of direct carbon removal. Through the remainder of the paper, we will refer to this counterfactual comparison as just the effect of emissions reductions.

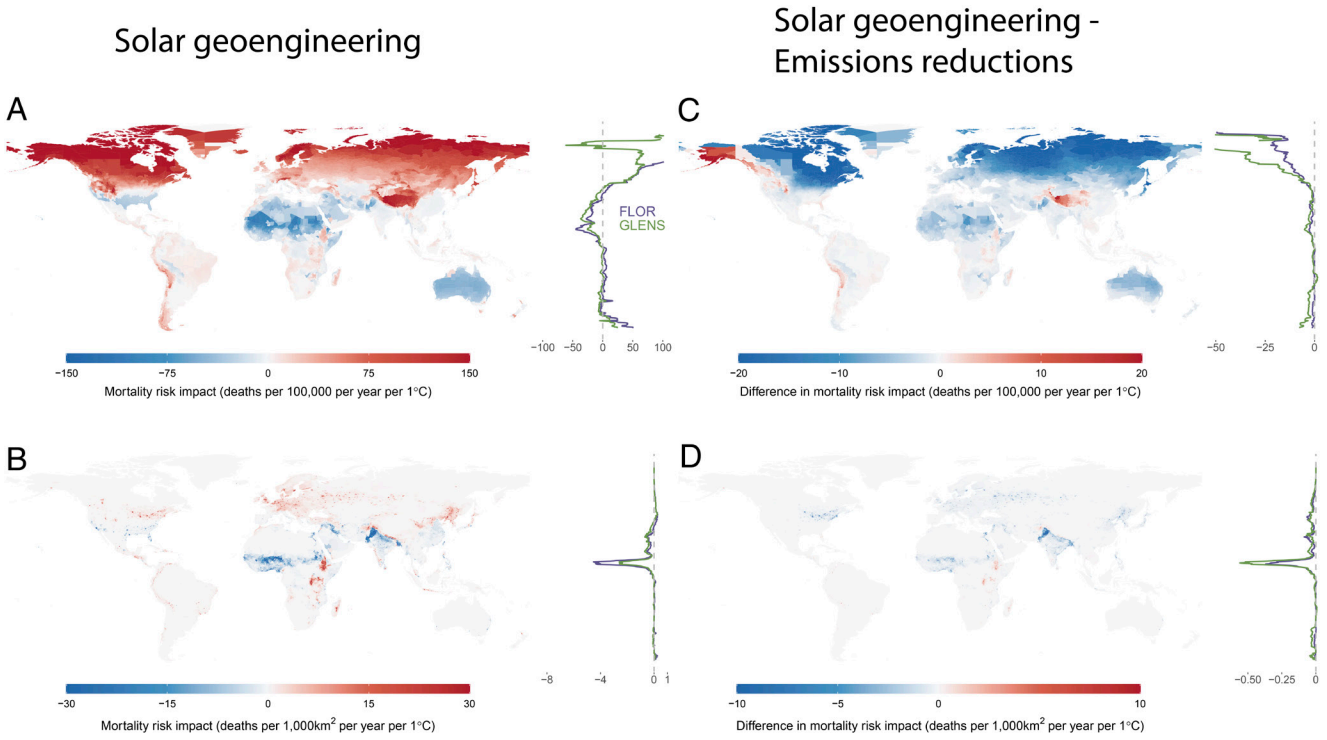

Fig. 1. Regional mortality rate impact with income growth and climate adaptation. Panels (*A*) and (*C*) show the impact of SG on temperature-attributable mortality. Blue indicates regions SG reduces mortality risk. Red indicates regions SG increases mortality risk. Panels (*B*) and (*D*) show the difference in mortality risk impact between SG and emissions reductions. Blue indicates regions where mortality risk is lower in a world cooled with SG. Red indicates regions where mortality risk is higher in a world cooled with SG. Panels (*A*) and (*B*) report impacts as deaths per 100,000 per year per 1 °C. Panels (*C*) and (*D*) report impacts as deaths per area per year, converting mortality rates to number of deaths using population in 2080. Maps present estimates for the FLOR climate model simulations. Zonal averages for both the FLOR and GLENS climate model simulations are shown to the right of each map. FLOR estimates assume income growth to 2080 and climate adaptation to each respective climate model experiment. Estimates for the GLENS climate model are averaged over the 2050–2059 decade with income growth and climate adaptation.

benefits more from cooling with emissions reductions when normalized per degree of global cooling (Fig. 1 *B* and *D* and *SI Appendix*, Table S1). This surprising result raises two obvious questions: why? And is the result robust? In the following sections we address the first question by analyzing differences in the climate response to SG and emissions cuts and the second question by examining the methodological assumptions and limitations of our analysis.

Climate Response. We compare the response of variables to SG relative to emissions reductions using a ratio r_X, defined as the ratio of change in variable X for SG relative to the change for emissions reductions, both normalized by the reduction in global mean temperatures (*Methods*). An $r_X > 1$ means a variable responds *more* strongly when global temperature is reduced by SG than when temperature is reduced by removing CO_2. An $r_X < 1$ means a variable responds *less* strongly to SG.

We consider daily average dry-bulb temperature, the driving variable for the empirically estimated mortality response of Carleton et al. (1) and most other heat-epidemiology studies (16). Perhaps the most striking characteristic is that SG cools equatorial regions more than emissions reductions and polar regions less (Fig. 2). This dampening of the equator-to-pole gradient, sometimes referred to as an "overcooling" of the tropics and undercooling of the poles, is a well-documented effect of globally uniform SG (17–19). If desired, this effect can be moderated through nonuniform SG that adjusts the latitudinal distribution of aerosol injection (20). Despite concerns about tropical overcooling, there is no objective sense in which uniform temperature reduction is the correct goal for SG. Given that a large fraction of the global population lives in equatorial regions, and the negative heath and productivity impacts of additional warming are strongest in these regions, utilitarian or justice concerns provide an argument for concentrating cooling in the tropics.

For annual average temperatures, median global population-weighted mean $r_{\overline{T}}$ is 1.087 (90% CI: [1.070,1.108]). This indicates that for equivalent global cooling, averaged over the places that people live, SG cools annual mean temperatures 8.7% more than emissions reductions. This is driven by an overcooling in latitudes ranging between 30°N to 40°S, where majority of the global population resides.

For heat extremes, median global population-weighted mean r_{THW} is 1.093 [90% CI: (1.028,1.180)]. Like annual average temperatures, SG tends to overcool heat extremes where people live relative to emissions reductions. This is consistent with previous analyses of the effect of SG on heatwaves (21). For cold extremes, r_{TCW} is 1.055 [90% CI: (0.988,1.153)]. SG leads to a relative overcooling of cold extremes in a much smaller latitudinal band range and undercools in more areas than for annual average temperature and heat extremes. Taken together, we find that SG reduces the intra-annual variability of temperatures in most populated regions of the world (*SI Appendix*, Fig. S5), and that this reduction in variability is larger than if the same global temperature reduction were achieved with CO_2 controls. Since temperature-attributable mortality is especially sensitive to extremes, this dampening of intra-annual variability is a mechanism through which SG may have a different impact than emissions reductions.

Now, let us return to the mortality projections from Fig. 1 and the question of why SG may have a greater impact on reducing temperature-attributable mortality risk than emissions reductions. The regional heterogeneity in SG's impact relative to emissions

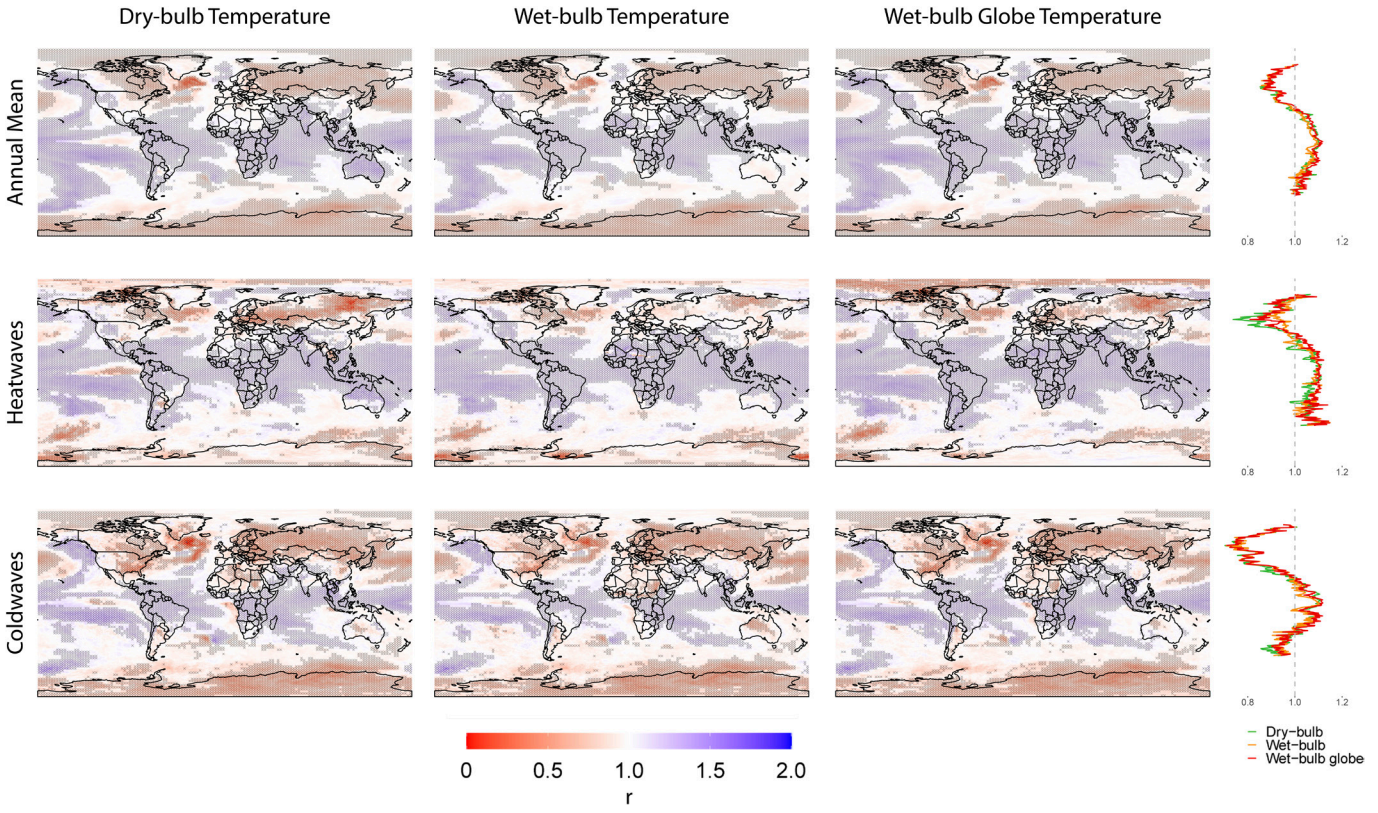

Fig. 2. Temperature response to SG relative to emissions cuts. Across columns from left to right we consider the response of dry-bulb temperature, wet-bulb temperature, wet-bulb globe temperature, and population-weighted zonal averages. Across rows from top to bottom we consider the response of annual mean temperature, heatwave intensity, and coldwave intensity. The intensity of cold (heat) extremes are measured as the 10th (90th) percentile of the rolling 5-d maximum (minimum) daily temperatures annually. Results for other percentiles can be found in *SI Appendix*, Figs. S3 and S4. Responses are measured using the ratio (r) that compares the effect of SG normalized per degree of global mean dry-bulb temperature change relative to the effect of emissions reductions normalized per degree of global mean dry-bulb temperature change. Displayed values are the median over 100 climate simulation years. Blue grid-cells indicate SG reduces temperatures more than emissions reductions and red grid-cells indicate SG reduces temperatures less than emissions reductions. Crosshatches indicate statistical significance at 90% confidence level using a Wilcoxon signed rank test corrected following the false discovery rate procedure. *Right*-hand subpanels show the population-weighted zonal average of the *Left*-hand subpanels.

reductions can broadly be explained by the heterogeneity in climate response of dry-bulb temperatures and whether regions benefit or are harmed by cooling. Equatorial regions generally benefit from cooling because reductions in heat-attributable mortality outweigh increases in cold-attributable mortality (Fig. 3). Since SG overcools these regions, they benefit more from SG than from emissions reductions. In the Global North, increases in cold-attributable mortality generally outweigh decreases in heat-attributable mortality (Fig. 3). Since SG undercools these regions, they benefit more from SG than from emissions reductions.

Limitations and Uncertainties. Our analysis is only as credible as our assumptions, of which our analysis has many. We now turn to the question of the robustness of our findings.

A key consideration in interpreting these results is the idealized nature of the forcing used in the climate model experiments. We explore the response to idealized CO_2 doubling experiments and idealized solar reduction experiment, each of which exclude potentially important aspects such a time evolution and spatial structure of forcing, and for the SG interpretation the impact of the agents used to reduction of insolation on atmospheric chemistry and physics. Future analyses should include a more comprehensive exploration of more realistic forcing on mortality.

Physiologically, heat stress is dependent not only on temperature but also on relative humidity and radiation (22), but our epidemiological model only uses dry-bulb temperature. One might expect errors to arise from applying that model to a world in which the correlations between temperature and relative humidity and radiation were different than they are in the current climate (23). For example, we expect that a world with SG will have higher relative humidity than a world with the same average temperature and no SG (24). Lacking an empirical model to quantify these effects, we analyze the climate response to SG for wet-bulb and wet-bulb globe temperatures at the surface, two composite measures of heat stress (*Methods*).

Compared with the response to dry-bulb temperature, we find that the distribution of the response of wet-bulb and wet-bulb globe is broadly similar (Fig. 2). The largest discrepancy is for heat extremes in northern regions where the relative undercooling of SG relative to emissions reductions is weaker for wet-bulb and wet-bulb globe temperatures. This, in turn, raises the population-weighted average ratio r_{THW} to 1.107 [90% CI: (1.073,1.129)] for wet-bulb temperature and 1.120 [90% CI: (1.108,1.166)] for wet-bulb globe temperature. These results suggest that a more complex empirical model of temperature-attributable mortality will have similar findings as for dry-bulb temperature or perhaps even find SG to be more effective.

In our projections above, we assume population distribution and income levels for 2080 because, if ever deployed, SG is unlikely to be deployed for several decades. Over that time, incomes are expected to grow and people will adapt to the newly experienced climate that may occur. For this reason, we also assume people have adapted to the climate of each respective climate model experiment. These assumptions affect the impact of SG on temperature-attributable mortality.

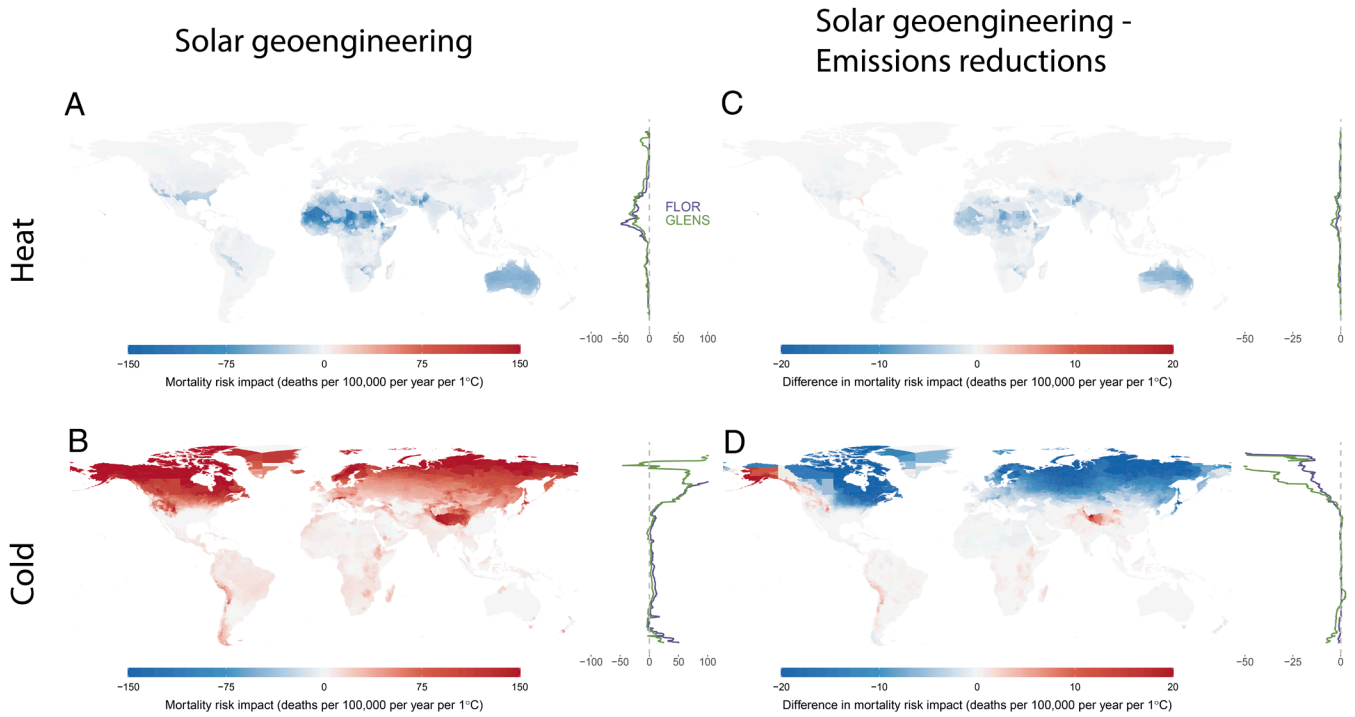

Fig. 3. Regional mortality rate impact by heat/cold with income growth and climate adaptation. Impact of SG on (*A*) heat-attributable mortality and (*C*) cold-attributable mortality. Blue indicates regions SG reduces mortality risk. Red indicates regions SG increases mortality risk. Difference in (*B*) heat-attributable and (*D*) cold-attributable mortality impact between SG and emissions reductions. Blue indicates regions where mortality risk is lower in a world cooled with SG. Red indicates regions where mortality risk is higher in a world cooled with SG. Impacts are reported as deaths per 100,000 per year per 1 °C. Maps present estimates for the FLOR climate model simulations. Zonal averages for both the FLOR and GLENS climate model simulations are shown to the right of each map. FLOR estimates assume income growth to 2080 and climate adaptation to each respective climate model experiment. Estimates for the GLENS climate model are averaged over the 2050–2059 decade with income growth and climate adaptation.

We re-estimate the projected impacts of SG under alternative assumptions. To constrain the effect of adaptation to changes in climate, we project mortality risk with income growth and adaptation to 1990 s climate (Inc Growth). To constrain the effect of income growth, we project mortality risk with income levels of 2015 and adaptation to 1990 s climate (No Adapt).

Allowing for only income growth dampens the global average impact of SG to a temperature-attributable mortality rate reduction of 10 per 1 °C [90% CI: (−7,29)] (Fig. 4*A*). Without income growth or climate adaptation, the impact is 21 per 1 °C [90% CI: (−3,48)]. Thus, income growth and capacity to adapt to climate changes clearly affect the magnitude of the temperature-attributable mortality impact of SG.

Comparing these estimates to the estimated mortality rate impact of emissions reductions, we find that with income growth but no climate adaptation SG reduces mortality rates by 1.4 [90% CI: (−1.1,4.0)] more than emissions reductions (Fig. 4*B*), an increase of 12% for the central estimates. Without income growth or climate adaptation, SG reduces mortality rates by 2.6 [90% CI: (−1.8,7.4)] more than emissions reductions, an increase of 14% for the central estimates. Thus, while income growth and climate adaptation reduce the impact of SG on temperature-attributable mortality, they have little to no effect on SG's impact relative to emissions reductions.

It is also possible that our estimates of the normalized impacts of SG and emissions reductions mechanically favors the impact of SG because temperature-attributable mortality is convex in changes in global mean temperature and a 1.7% solar constant reduction does not fully revert the change in global mean temperature from a doubling of CO_2 concentrations (*SI Appendix*, Fig. S1*C*). To correct for this, we select a subset of 47 simulation years in which global mean temperatures for the control and 2xCO_2&SG scenarios overlap, so that the change in global mean temperature is more comparable. Considering only these simulation years, SG's mortality rate impact is 3 per 1 °C [90% CI: (−10,24)] and compared to emissions reduction, SG reduces mortality rates by 1.2 per 1 °C [90% CI: (−0.8,3.9)] more. As above, these estimates use population and income for SSP3 in 2080 with climate adaptation to the climate of each respective experiment. The reduction in both the mortality rate impact and difference in mortality rate impacts compared with emissions reductions reflect the nonlinearity of the sensitivity of mortality rates to changes in global mean temperature, however the consistency of these results with the unconstrained results suggest that the nonlinearities in impacts are not driving our findings.

Any simulation of stratospheric aerosol SG carries two kinds of uncertainty. First is uncertainty about policy choices—which type and how much aerosol is deployed, and how it is distributed. Given the strong effects of shifting the Intertropical Convergence Zone (ITCZ), we assume that any politically stable deployment would aim at balancing between the northern and southern hemispheres. This still leaves a nonobvious policy choice about how much and which aerosol to deploy and how to address cooling of the tropics versus the poles. Second, all climate models have substantial limitations and there are trade-offs between model capabilities.

Our analysis above focuses on the FLOR model, driven by a uniform solar constant reduction. The advantage of the FLOR model is that its higher spatial resolution and longer time horizon provide better representation of extremes and reduce uncertainties from internal variability. A disadvantage of this experimental setup is that reducing insolation does not treat the stratospheric impacts of stratospheric sulfate (or other) aerosols such as stratospheric heating (25, 26). Here, we use the Stratospheric Aerosol Geoengineering Large Ensemble project simulations (GLENS) (27). The control simulations of GLENS follow a RCP8.5 emissions scenario. In the

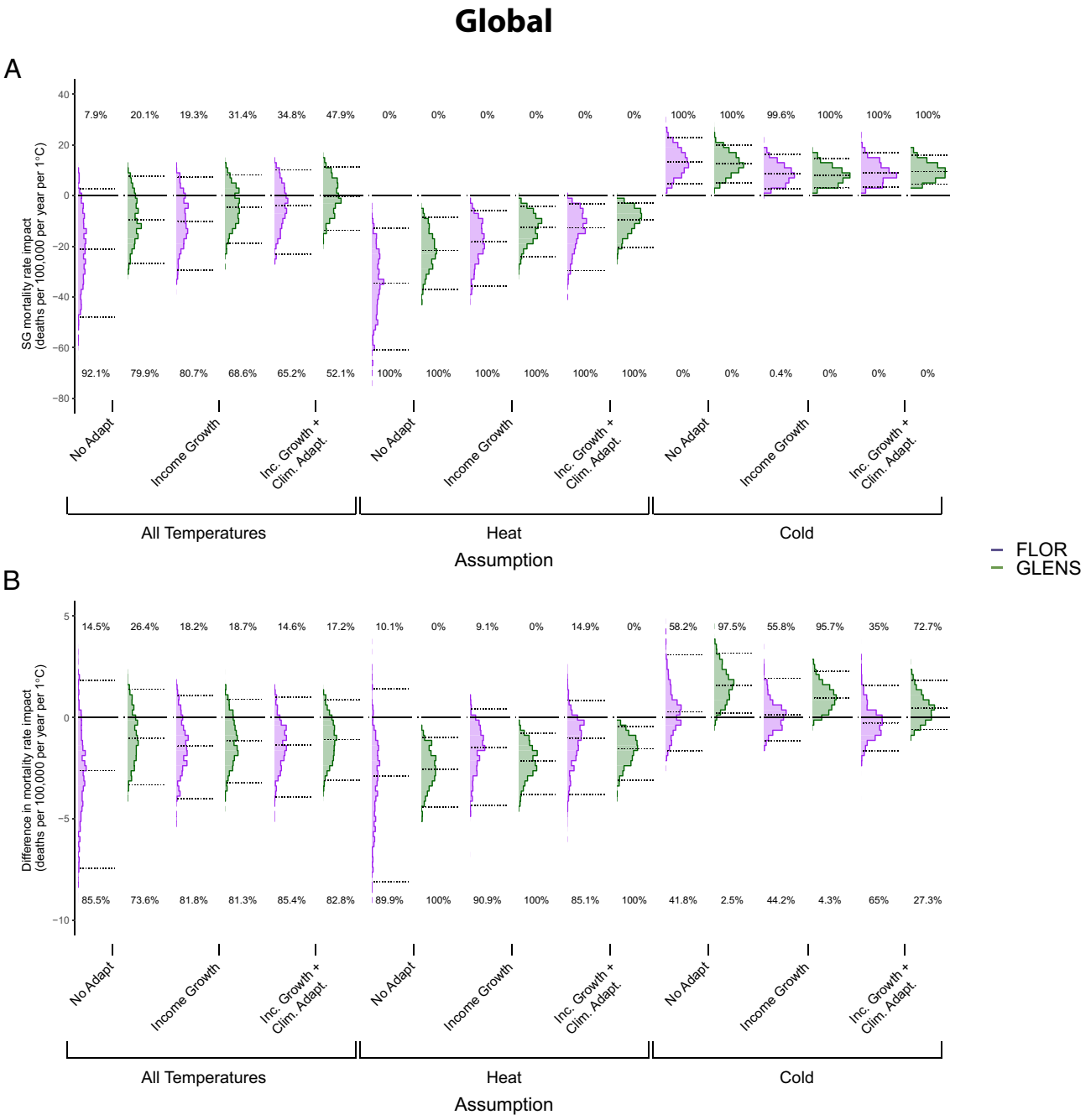

Fig. 4. Uncertainty in global mortality rate impact. (*A*) Distribution of estimates of global mortality rate impact of SG normalized per degree of global mean cooling across climate model simulations and adaptation assumptions. (*B*) Distribution of estimates of difference in global mortality rate impact for SG relative to emissions reductions normalized per degree of global mean cooling across climate model simulations and adaptation assumptions. FLOR climate model estimates use SSP3 2080 population and SSP3 income for 2015 with no income growth and 2080 with income growth. Estimates for the GLENS climate model are averaged over the 2050 to 2059 decade and use SSP3 population and income. For each distribution of estimates, the middle dotted line denotes the median estimate and the upper and lower dotted lines denote the 90% CI. Numbers above and below distributions denote the percentage of estimates above and below 0, respectively.

SG simulations of GLENS, SG is driven by stratospheric aerosol injection at four latitudes aimed to maintain multiple temperature targets, including the equator-to-pole gradient (*Methods*). The advantage is that the atmospheric component of the GLENS simulations, WACCM, has a high-quality representation of stratospheric dynamics. A disadvantage is that lower resolution and shorter integration time limit the ability to model changes in extremes.

For the control scenario, which follows RCP8.5 forcings, global mortality risk increases convexly over the century (*SI Appendix*, Fig. S10). To compare estimates with those from the FLOR model, we focus on the 2050 to 2059 decade where global mean cooling from SG is comparable to the FLOR model (*SI Appendix*, Table S2) and we do not include costs of adaptation. We estimate the normalized mortality rate impact of SG is 0.1 per 1 °C [90% CI: (−9,10)] with income growth and climate adaptation.[‡] We find the normalized mortality rate impact of SG increases over time and when we do not allow for income growth or climate adaptation (Fig. 4 and *SI Appendix*, Table S2). This indicates that the impact of SG depends considerably on the context in which it is deployed.

[‡]This rises to 4 per 1 °C [90% CI: (−8,19)] when including the costs of adaptation. For the remainder, we do not consider adaptation costs for the GLENS projections since they cannot be calculated for the FLOR projections.

Compared with FLOR, estimates of the impact of SG on temperature-attributable mortality rates for GLENS are smaller but also more uncertain. GLENS adjusts the latitudinal distribution of injection to better manage the change in the pole-to-equator gradient, i.e. the overcooling of the equatorial region is not as strong for the GLENS simulations. This reduces the impact of SG which is strongest in equatorial regions. Uncertainty is larger for the GLENS estimates than for the FLOR model due to a shorter time integration. However, we find no evidence that SG reduces temperature-attributable mortality by less than emissions reductions for GLENS, as with FLOR. Comparing SG to emissions reductions, we find that mortality rates are reduced by 1.0 per 1 °C [90% CI: (–1.6,4.1)] more with SG, consistent with estimates for the FLOR model (Fig. 4*B*). We estimate that SG reduces mortality rates by 1.1 [90% CI: (–1.7,4.1)] per 1 °C more than emissions reductions with income growth but no climate adaptation and by 1.0 [90% CI: (–3.2,5.2)] more with no income growth or climate adaptation.

Toward a Risk–Risk Comparison. We find that SG can moderate the temperature-attributable mortality risk of climate change. Yet, SG also introduces novel risks. Recent research on SG highlights the urgent need for risk–risk comparisons as a guide for climate policy decision-making (4–6, 28). Here, we take a small but important first step toward a more comprehensive quantitative risk–risk assessment by comparing our estimates of the impact of SG on temperature-attributable mortality to estimates of the direct human mortality risk from sulfate aerosol geoengineering.

Sulfate aerosol injection will deplete stratospheric ozone and add particulate matter (PM) to the lower atmosphere altering mortality from exposure to UV-B, PM, and ozone. For SG which offsets global mean temperature by 1 °C in 2040, these changes are estimated to increase net mortality by 26,000 deaths per year [90% CI: (–19,000 to 73,000)] (7). For a global population of 9 billion in 2040, this is 0.3 per 1 °C [90% CI: (–0.2,0.8)]. For the FLOR model with income growth and climate adaptation, we find that SG reduces temperature-attributable mortality rates by 4 per 1 °C [90% CI: (–10,23)]. Comparing mean estimates, the benefits of reduced temperature attributable mortality outweigh the risks by a factor of around 13. Incorporating uncertainty in estimates (*Methods*), we find the median net impact of SG on mortality rates is a reduction of 4 per 1 °C [90% CI: (–11,23)] (*SI Appendix*, Fig. S14). Across our Monte Carlo simulations, we find with 61.3% probability that SG would reduce morality rates when weighing the temperature-attributable mortality benefits against the direct mortality risks. Uncertainty in the net impacts of SG is dominated by uncertainty in estimates of SG's impact on temperature-related morality, as is evidenced by the finding that the probability SG reduces temperature-attributable mortality—neglecting the sulfate aerosol impacts—is almost the same at 65.2%. For GLENS, we find the net impact of SG on mortality rates is an increase of 2 per 1 °C [90% CI: (–13,11)] for the 2040 s decade. This decreases over time to a reduction of 8 per 1 °C [90% CI: (–7,25)] by the end of the century (*SI Appendix*, Fig. S15). While this compares only a few of the risks of SG, air quality and heat are plausibly two of SG's largest impacts on mortality.

There are uncertainties in both sources of mortality risk, and thus in our risk–risk comparison. Many uncertainties are captured in the CI of the two analyses, but others are not. The net mortality impact computed in Eastham et al. (7) combines the direct impacts of the injected aerosol with indirect effects from the change in radiative forcing that changes climate that changes the amount of surface ozone and PM produced from given emissions of precursors, such as NO_X and SO_2. Eastham et al. uses 2040 precursor emissions, but if a 1 °C cooling from SG occurs late this century, then precursor emissions will likely be lower and these indirect effects smaller. It may be better to compare our temperature-attributable mortality estimate to Eastham et al. (7) estimate of direct impacts of the descending injection mass [7,400 deaths per year, 90% CI: (2,500 to 12,300)] and the added UV-B mortality [4,100 deaths per year, 90% CI: (1,200 to 7,000)]. This yields a combined mortality rate of around 0.1 for a population of 9 billion, and a correspondingly higher benefit to risk ratio. Uncertainty in estimates of this benefit-risk ratio could be improved with a more consistent modeling framework for both temperature and atmospheric chemistry.

Discussion

Human mortality risk from extreme weather is a major risk of climate change. We find that SG could substantially reduce temperature-attributable mortality risk. Further, we find no evidence that, for equivalent global cooling, SG moderates this risk less than the counterfactual impact of emissions reductions. If anything, SG may reduce mortality risk by moderately more. This is due to differences in the climate response between SG and emissions reductions—particularly a reduction in intra-annual temperature variability and relative cooling of the most sensitive equatorial regions. There is regional heterogeneity. Broadly, regions in the Global South tend to benefit from cooling while risk increases in regions in the Global North. Our results are robust to a variety of alternative assumptions about socioeconomics, adaptation, and climate modeling.

A salient concern about SG is the uneven distribution of its impacts. While there is considerable evidence that SG can moderate climate changes globally, there is concern about its regional impacts and whether it will have different impacts on countries with different wealth. Comparing across levels of regional wealth, we find that the beneficial impact of SG on temperature-attributable mortality is strongest for the least wealthy regions (Fig. 1). Intuitively, if we posit that climate vulnerability has some inverse relationship to wealth, that is the least wealthy regions are the most sensitive to the impacts of a warming climate, cooling these regions could have a disproportionate impact in reducing climate risk. Further, we find no evidence that SG performs worse than emissions reductions at reducing temperature-attributable mortality across any of the income deciles.

Emissions cause long-term climate and geochemical risks that SG cannot abate, so SG cannot substitute for emissions reductions. Our results do suggest that SG supplement emissions reductions by moderating an important impact of climate change on human mortality and that the countervailing mortality risks examined so far are comparatively small. Our work is just a step toward a broad quantitative risk–risk assessment of SG. Yet we caution that quantitative risk–risk assessment cannot capture many important concerns about SG so a favorable risk–risk ratio cannot serve as a sufficient justification for decisions about deployment.

Methods

GFDL FLOR. The GFDL FLOR model uses a high-resolution (50 km) atmosphere and land component taken from the Coupled Model, v.2.5 (CM2.5) and a lower-resolution (1°) ocean and sea ice complement taken from the Coupled Model, v.2.1 (CM2.1). Full details of the GFDL FLOR model can be found in Vecchi et al. (12).

For GFDL FLOR, a control simulation is run for 300 y with conditions of 1990. The $2xCO_2$ experiment and solar dimming experiments branch off the control

simulation in year 101 and run for 200 years. In the $2xCO_2$ experiment, atmospheric concentrations of CO_2 are doubled from the control simulation. In the solar dimming experiment, atmospheric concentrations of CO_2 are doubled from the control simulation and the solar constant is reduced by 1.7%. We use the last 100 years of each simulation for our analyses.

GLENS. The GLENS simulations are modeled using the NCAR Community Earth System Model, v.1 (CESM1), with the Whole Atmosphere Community Climate Model (WACCM) for the atmosphere component. Full details of the GLENS simulations can be found in Tilmes et al. (27).

For the GLENS simulations, the control simulations use the greenhouse gas forcing concentrations for RCP 8.5 from 2010 through 2099. The SG simulations use RCP 8.5 concentrations with SO_2 injection at four latitudes–30 N, 30S, 15 N, and 15S–beginning in 2020. Aerosol injection is adjusted following a feedback-control algorithm to simultaneously minimize deviations in global mean surface temperature, interhemispheric temperature gradient, and the equator-to-pole temperature gradient from 2020 values. For our analyses, we use the 3 control and corresponding SG ensemble members that run to the end of the century.

Normalization. Throughout the analysis, we normalize climate response and mortality risk impacts by the change in global annual mean temperature. For example, the normalized response of a given variable X to SG is given as

$$< X^{2xCO2} - X^{SG} > \; = \frac{X^{2xCO_2} - X^{SG}}{\overline{T}^{2xCO_2} - \overline{T}^{SG}},$$

where $\overline{T}$ is the global annual mean temperature. This captures the change in the variable X per degree of global mean temperature cooling from SG. This is equivalent to linearizing the response of variable X to the change in global annual mean temperature. This can be calculated for changes in X at the grid-cell level or globally.

From this normalization, we introduce a ratio metric r to compare the effects of SG and emissions reductions. For a given variable X, the ratio r_X is given as

$$r_X = \frac{< X^{2xCO2} - X^{SG} >}{< X^{2xCO2} - X^{CTL} >}.$$

The ratio metric can also be calculated either at the grid-cell level or globally. The accuracy of this normalization and ratio approach depends on the assumption that responses are approximately linear in the change in global mean surface temperature. While we do not test this assumption here, it is found to be a valid assumption for a range of climate variables in other settings (29).

Empirical Estimated Impact. Temperature-attributable mortality risk estimates follow the methodology outlined in Carleton et al. (1). Here, we describe the key estimation methods for our analysis. For a more comprehensive description see Carleton et al. (1). We use the 24,378 impact regions, each around the size of a US county, and the corresponding calibrated SSP income and population data constructed in their analysis.

We estimate mortality impacts for each simulation year by integrating region- and age-specific dose–response curves–which describe the relationship between temperature and mortality rates–over daily temperatures. Dose–response curves are constructed using the coefficients and covariance matrix for the econometric estimation of the historical temperature-mortality relationship from Carleton et al. (1). The estimates relate mortality rates to temperature interacted with regions' climate and income, captured by Equation (4) in their text. We follow the procedures outlined in their *SI Appendix*, section E to define the minimum mortality temperature and correct the dose–response curves.

For our baseline estimates, we fix the income covariate as the Bartlett kernel of income for SSP3 in 2015 with a length of 13 y. For the GFDL FLOR climate simulations, we fix the climate covariate as the average of annual mean temperature for the last 100 control simulation years. For GLENS climate simulations, we fix the climate covariate as the Bartlett kernel of annual mean temperature in 2015 with a length of 30 y. To analyze the effect of income growth, we alternatively use the Bartlett kernel of income for SSP3 in 2080. To analyze the effect of climate adaptation, for the GFDL FLOR climate simulations, we use the average of annual mean temperature for the last 100 simulation years in each respective experiment. We do not estimate adaptation costs for these projections. Measurement of adaptation costs as laid out in Carleton et al. (1) requires continuous marginal changes in climate, measured as changes in a 30-year weighted average. Thus, we cannot apply this methodology to the FLOR climate model experiments where the changes in climate are a large discrete change. For the GLENS climate simulations, we allow the Bartlett kernel of annual mean temperature to evolve over time. To be consistent with the FLOR estimates and focus on the physical mortality risk impacts, we again do not account for adaptation costs. The only exception is in *SI Appendix*, Figs. S10*B* and S11 where we include adaptation costs when comparing our estimates to the estimates of Carleton et al. (1) for benchmarking. For the GFDL FLOR model, impacts are aggregated using population weights for the SSP3 scenario in 2080, a more realistic year for SG to be implemented with a 1 °C magnitude. For the GLENS model, impacts are aggregated using population weights for the SSP3 scenario in each respective year. In *SI Appendix*, section 1 - Alternative SSPs, we present alternative results for SSP2 and SSP5 with the FLOR simulations.

We account for uncertainty both in the econometric estimates and the climate simulations using Monte Carlo simulations. To account for econometric uncertainty, we randomly sample coefficients for the econometric parameters using a multivariate normal distribution characterized by the covariance matrix between all the parameters. To account for climate uncertainty in the GFDL FLOR model we randomly draw simulation years. To account for climate uncertainty in the GLENS simulations, we randomly draw ensemble members. This process of randomly drawing a set of coefficients and a model year or an ensemble member is repeated 1,000 times.

Downscaling and Bias-Correction. To mitigate concerns of stationary biases (30) in our empirical analysis of temperature-attributable mortality we downscale and bias-correct both the GFDL FLOR and GLENS climate simulation output. First, minimum and maximum daily 2 m temperature is downscaled to a 0.25° x 0.25° spatial resolution using bilinear interpolation. Next, downscaled temperature is bias-corrected to the GMFD data (8) used to empirically estimate historical dose–response functions. Data are bias corrected following the ISI-MIP method (31). For the GFDL FLOR, the first 10 years of the control scenario is matched to the GMFD data for 1990 to1999 since the control is set to 1990s conditions. For the GLENS model, years 1980 to 2010 are matched to the corresponding years in the GMFD data. Finally, we calculate daily average temperature for each of the impact regions as the population-weighted mean of daily maximum and minimum temperature. Population-weights come from LandScan Global 2011 (32).

Wet-Bulb and Wet-Bulb Globe Temperature. Wet-bulb temperature (Tw) is calculated as a function of ambient temperature (T_a) and relative humidity ($RH\,\%$) using the following approximating formula developed by Stull (2011) (33),

$$Tw = T_a \;\mathrm{atan}\left[0.151977(RH\% + 8.313659)^{\frac{1}{2}}\right] + \mathrm{atan}\left(T_a + RH\%\right) - \mathrm{atan}(RH\% - 1.676331) + 0.00391838(RH\%)^{\frac{3}{2}}\mathrm{atan}(0.023101RH\%) - 4.686035.$$

This formula is accurate for relative humidity ranging from 5% to 99% and for ambient temperature ranging from −20 °C to 50 °C, except for both low humidity and cold temperature.

Wet-bulb globe temperature (WBGT) is a linear combination of ambient temperature (T_a), natural wet-bulb temperature (T_w), and black globe temperature (T_g), given as

$$\mathrm{WBGT} = 0.1T_a + 0.7T_w + 0.2T_g.$$

To calculate wet-bulb globe temperature, we follow the model of Liljegren et al. (2008) (34) using code developed by Kong and Huber (2022) (35).

Risk–Risk Comparison. To compare our estimates of the impact of SG on temperature attributable mortality to the direct mortality risks of SG estimated in Eastham et al. (7), we first reconstruct an uncertainty distribution for the estimates of Eastham et al. (7) by fitting a normal distribution to their reported mean estimates and 95% CI. Intervals reported in the text come from the fit distribution. We then randomly sample 1,000 draws from our Monte Carlo estimates of mortality rate impacts and from the reconstructed mortality risk estimates of Eastham et al. (7) and compare (*SI Appendix*, Figs. S14 and S15).

Data, Materials, and Software Availability. Replication data and code are available at (36).

ACKNOWLEDGMENTS. A.H. and D.W.K. acknowledge support from the LAD Climate Fund. G.A.V. and W.Y. acknowledge support from US Department of Energy Grant DE-SC0021333 and funding support from the Simons Foundation. We thank Kevin Cromar and other participants in workshops at Resources for the Future for useful comments and feedback. We thank Simone Tilmes for assistance in accessing GLENS simulation data. We thank Antonella Zanobetti and Joel Schwartz for helpful conversations in early stages of the project.

Author affiliations: [a]School of Public Policy, Georgia Institute of Technology, Atlanta, GA 30032; [b]Department of Geosciences, Princeton University, Princeton, NJ 08544; [c]High Meadows Environmental Institute, Princeton University, Princeton, NJ 08544; and [d]Department of Geophysical Sciences, University of Chicago, Chicago, IL 60637

1. T. Carleton *et al.*, Valuing the global mortality consequences of climate change accounting for adaptation costs and benefits. *Q. J. Econ.* **137**, 2037–2105 (2022).
2. S. Hsiang *et al.*, Estimating economic damage from climate change in the United States. *Science* **356**, 1362–1369 (2017).
3. K. Rennert *et al.*, Comprehensive evidence implies a higher social cost of CO2. *Nature*, **610**, 687–692 (2022). 10.1038/s41586-022-05224-9.
4. A. R. Harding, M. Belaia, D. W. Keith, The value of information about solar geoengineering and the two-sided cost of bias. *Clim. Policy*, **23**, 355–365 (2022).
5. T. Felgenhauer *et al.*, Solar radiation modification: A risk-risk analysis (Carnegie Climate Governance Initiative (C2G), 2022). https://scholars.duke.edu/display/pub1508823. Accessed 14 November 2022.
6. E. A. Parson, Geoengineering: Symmetric precaution. *Science* **374**, 795–795 (2021).
7. S. D. Eastham, D. K. Weisenstein, D. W. Keith, S. R. H. Barrett, Quantifying the impact of sulfate geoengineering on mortality from air quality and UV-B exposure. *Atmos. Environ.* **187**, 424–434 (2018).
8. H. Kuswanto *et al.*, Impact of solar geoengineering on temperatures over the Indonesian Maritime Continent. *Int. J. Climatol.* **42**, 2795–2814 (2022).
9. C. J. Carlson *et al.*, Solar geoengineering could redistribute malaria risk in developing countries. *Nat. Commun.* **13**, 2150 (2022).
10. J. Moreno-Cruz, K. L. Ricke, D. W. Keith, A simple model to account for regional inequalities in the effectiveness of solar radiation management. *Clim. Change* **110**, 649–668 (2012).
11. E. A. Parson, D. W. Keith, Solar geoengineering: History, methods, governance, prospects. *Annu. Rev. Environ. Resour.* **49**, 337–366 (2024). 10.1146/annurev-environ-112321-081911.
12. G. A. Vecchi *et al.*, On the seasonal forecasting of regional tropical cyclone activity. *J. Clim.* **27**, 7994–8016 (2014).
13. K. van der Wiel *et al.*, The resolution dependence of contiguous U.S. precipitation extremes in response to CO2 forcing. *J. Clim.* **29**, 7991–8012 (2016).
14. S. Y. Philip *et al.*, Rapid attribution analysis of the extraordinary heatwave on the Pacific Coast of the US and Canada June 2021. *Earth Syst. Dyn. Discuss.* **13**, 1689–1713 (2021). 10.5194/esd-2021-90.
15. United Nations, Department of economic and social affairs, population division. world population prospects: The 2022 revision. *World Population Prospects: The 2022 Revision* (2022). https://population.un.org/wpp/.
16. B. Armstrong *et al.*, The role of humidity in associations of high temperature with mortality: A multicountry, multicity study. *Environ. Health Perspect.* **127**, 097007 (2019).
17. B. Govindasamy, K. Caldeira, Geoengineering Earth's radiation balance to mitigate CO2-induced climate change. *Geophys. Res. Lett.* **27**, 2141–2144 (2000).
18. G. A. Ban-Weiss, K. Caldeira, Geoengineering as an optimization problem. *Environ. Res. Lett.* **5**, 034009 (2010).
19. P. J. Irvine, B. Kravitz, M. G. Lawrence, H. Muri, An overview of the Earth system science of solar geoengineering. *Wiley Interdiscip. Rev. Clim. Change* **7**, 815–833 (2016).
20. B. Kravitz *et al.*, Comparing surface and stratospheric impacts of geoengineering with different SO2 injection strategies. *J. Geophys. Res. Atmos.* **124**, 7900–7918 (2019).
21. K. Dagon, D. P. Schrag, Regional climate variability under model simulations of solar geoengineering. *J. Geophys. Res. Atmos.* **122**, 12106–12121 (2017).
22. J. R. Buzan, M. Huber, Moist heat stress on a hotter earth. *Annu. Rev. Earth Planet. Sci.* **48**, 623–655 (2020).
23. A. R. Harding, K. Ricke, D. Heyen, D. G. MacMartin, J. Moreno-Cruz, Climate econometric models indicate solar geoengineering would reduce inter-country income inequality. *Nat. Commun.* **11**, 227 (2020).
24. K. Ricke, J. S. Wan, M. Saenger, N. J. Lutsko, Hydrological consequences of solar geoengineering. *Annu. Rev. Earth Planet. Sci.* **51**, 447–470 (2023).
25. D. Visioni, D. G. MacMartin, B. Kravitz, Is turning down the sun a good proxy for stratospheric sulfate geoengineering? *J. Geophys. Res. Atmospheres* **126**, e2020JD033952 (2021).
26. E. M. Bednarz *et al.*, The overlooked role of the stratosphere under a solar constant reduction. *Geophys. Res. Lett.* **49**, e2022GL098773 (2022).
27. S. Tilmes *et al.*, CESM1(WACCM) stratospheric aerosol geoengineering large ensemble project. *Bull. Am. Meteorol. Soc.* **99**, 2361–2371 (2018).
28. J. E. Aldy *et al.*, Social science research to inform solar geoengineering. *Science* **374**, 815–818 (2021).
29. B. Kravitz *et al.*, A multi-model assessment of regional climate disparities caused by solar geoengineering. *Environ. Res. Lett.* **9**, 074013 (2014).
30. M. Auffhammer, S. M. Hsiang, W. Schlenker, A. Sobel, Using weather data and climate model output in economic analyses of climate change. *Rev. Environ. Econ. Policy* **7**, 181–198 (2013).
31. S. Hempel, K. Frieler, L. Warszawski, J. Schewe, F. Piontek, A trend-preserving bias correction–the ISI-MIP approach. *Earth Syst. Dyn.* **4**, 219–236 (2013).
32. E. Bright, P. Coleman, A. Rose, M. Urban, LandScan Global 2011 (Oak Ridge National Laboratory, 2012). 10.48690/1524207. Accessed 5 September 2022.
33. R. Stull, Wet-bulb temperature from relative humidity and air temperature. *J. Appl. Meteorol. Climatol.* **50**, 2267–2269 (2011).
34. J. C. Liljegren, R. A. Carhart, P. Lawday, S. Tschopp, R. Sharp, Modeling the wet bulb globe temperature using standard meteorological measurements. *J. Occup. Environ. Hyg.* **5**, 645–655 (2008).
35. Q. Kong, M. Huber, Explicit calculations of wet-bulb globe temperature compared with approximations and why it matters for labor productivity. *Earths Future* **10**, e2021EF002334 (2022).
36. A. Harding *et al.*, Replication data for: Impact of solar geoengineering on temperature-attributable mortality. OSF. https://doi.org/10.17605/OSF.IO/JZY3G. Accessed 9 September 2024.